Consequences of Simplifications in Modelling and Analysis of Masonry Arch Bridges

Tomasz Kamiński(✉)

Wrocław University of Science and Technology, Wybrzeże Wyspiańskiego 27, 50-370 Wrocław, Poland
tomasz.kaminski@pwr.edu.pl

Abstract. The paper presents a problem of a simplified modelling of masonry arch bridges utilising a linear elastic material model. Although, such approach provides significant time and labour savings, it may lead to dangerous overestimation of the load carrying capacity of evaluated structures. Theoretical bases for this effect are being explained and illustrated by means of a comparison of two essentially different approaches to analysis of masonry arch bridges. Both of them are using Finite Element Method, however each with different material model for the arch barrel. One of them is based on an advanced nonlinear non-tensile-resistant constitutive model most properly representing masonry, while the other one is a linear-elastic model with unlimited compressive as well as tensile strength. In a parametric study of bridges with various geometries and mechanical properties all differences depending on the applied material model in the structures' response to typical loading scenario are presented. Clear measures enabling numerical comparison of the approaches are given. Some diagrams are provided to describe and explain effectively the essence and causes of the appearing differences (including distribution of internal forces or cracking development) originating from the chosen material modelling techniques. General conclusions coming from the study are drawn.

Keywords: Masonry arch bridge · Numerical modelling · Nonlinear analysis · The ultimate load

1 Introduction

There are many approaches to analysis of masonry arch bridges. The first of them were discovered before ages while the latest ones are still being developed in XX1 century. The earlier methods were based on numerous simplifications which currently can be avoided utilising contemporary advanced models and computer techniques. The modern and the most accurate approaches are however more time-consuming and labour demanding what leads often to selection of simpler models for analysis of masonry arch bridges even nowadays (also predicted by official recommendations [1]). A serious problem potentially caused by such a simplification is related to dangerous overestimation of the load carrying capacity of evaluated structures.

The paper is going to depict the aforementioned problem by means of comparison of two essentially different approaches to analysis of masonry arch bridges. Both of

A. Arêde and C. Costa (Eds.): ARCH 2019, SI 11, pp. 153–160, 2020.
https://doi.org/10.1007/978-3-030-29227-0_12

them are using Finite Element Method, however each with different material model for the arch barrel.

2 The Applied Models

2.1 General Description

Two-dimensional Finite Element plane model of a masonry bridge representing: the arch barrel, the soil above the arch barrel and in the access zones, pavement layer and a loading element is adopted in the analyses (see Fig. 1). The model is defined as a plane-strain problem and it represents a unit width of the bridge structure what is a standard procedure validated by means of numerous laboratory and field tests [2–6]. Except its self-weight the bridge is subjected to an external loading simulating a pressure of a single axle of a vehicle increasing gradually up to the ultimate load level.

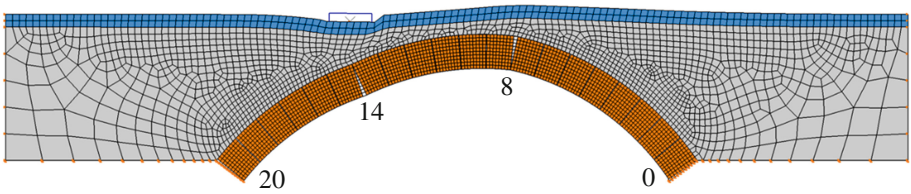

Fig. 1. FE model of a masonry arch bridge applied in analyses (deformed shape at the ultimate load level)

2.2 Details of the Numerical Model

The arch barrel is modelled as a continuous area defined by means of two types of material model: an advanced nonlinear (NL) elastic-plastic at compression non-tensile-resistant constitutive model – the most precisely representing masonry, while the other one is a linear-elastic (EL) model with unlimited compressive as well as tensile strength. In the first case a meso-modelling technique [7, 8] is used which is based on division of the arch barrel area into masonry segments with homogenised properties, comprising groups of several masonry blocks together with the joints between them, and into layers of radial joints between the segments. The segments are modelled by means of an orthotropic material representing average characteristics of its components, i.e. determined by a homogenized stiffness matrix combining average strains and average stresses within the segments [7]. The selected radial joints (between the masonry segments) are those areas where cracking may occur forming the typical failure mode of the arch, therefore they are modelled with special care. The material of the joints defined as a plastic-damage model (proposed in [9, 10]) corresponds to the constitutive model of concrete. A simplified representation of σ-ε relationship for uniaxial behaviour of the mortar material is presented in (Fig. 2).

The branches covering compression and tension outside the linear elastic range of σ-ε relationship are precisely determined by means of strain hardening/softening

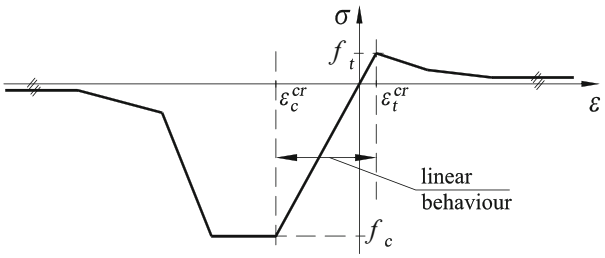

Fig. 2. σ-ε relationship for uniaxial behaviour defining concrete-like material model of mortar

curves. The initial yield stresses at tension and compression are equal to typical values [11]: f_t = 0.1 MPa and f_c = 4 MPa correspondingly, while they are being reduced to about one order lower values at extremities of the diagram in Fig. 2.

The other main material properties of material assumed in analyses valid also for linear-elastic model are shown in Table 1 where: $\gamma_{M/pav}$, γ_f – unit weights of masonry/pavement and backfill; E_m, E_b, E_f, E_p – modulus of elasticity of mortar, bricks, backfill and pavement; c – cohesion of the backfill; ϕ – angle of internal friction of the backfill, μ – coefficient of friction between the arch barrel and the soil.

Table 1. Material properties of the analysed bridges

Parameter	$\gamma_{M/pav}$ kg/m^3	γ_f kg/m^3	E_b GPa	E_m GPa	E_f MPa	E_p MPa	ϕ deg	c -	μ -
Value	2000	1850	10	1.0	50	100	45	10	0.4

At the boundary between the backfill and the arch the contact elements are defined. They represent interaction between the contacting bodies by means of compressive and shear forces but without transfer of tension.

The live load is applied by means of a rigid block acting on the upper edge of the pavement (see Fig. 1). In all analyses the load is located at the quarter of the span. The boundary conditions limit the horizontal translation of the rigid body.

2.3 Analysis Procedure

The solution is carried out incrementally in two consecutive steps: in the first one self-weight of all structural components is applied, in the second one the live load acting through the rigid block is added. The incremental application of the live load is determined by means of the vertical displacement of the loading block, what gives better control over the loading process and development of the global failure. Thus, the ultimate load level P_{ult} may be reached what is defined by the highest value of the applied load taken from the relationship between the vertical displacement u of the loading block and the concentrated force P equal to the reaction acting on the block.

3 Parametric Study

3.1 Considered Cases

The basic geometrical parameters of the analysed bridges are presented in Table 2, where L – arch clear span; r/L – rise-to-span ratio; d – arch thickness; N – number of arch segments, h – backfill height over the crown; w – length of the loading block. In total 4 various cases are considered varying in arch rise and thickness.

Table 2. Geometrical parameters considered in the parametric study

Parameter	L [m]	r/L [-]	d [m]	N [-]	h [m]	w [m]
Values	5.0	1/4; 1/8	0.25; 0.40	20	0.3	0.5

3.2 Results

The analysis is oriented on evaluation of the differences between EL and NL models on the basis of results including: relationship between stresses σ_x in critical sections and force P applied to the bridge (Fig. 3), thrust eccentricity e (Fig. 4), distribution of stresses σ_x along both edges of the arch (Fig. 5) as well as throughout the critical sections (Fig. 6) numbered according to Fig. 1. The aforementioned results given in the figures are for case of an arch with f/L = 1/4 and d = 40 cm. Furthermore, specific three phases of the bridge loading are considered:

1. phase I – at force P_I level corresponding to reaching by the edge stresses the compressive strength f_c in the NL model,
2. phase II – at force $P_{II} = P_{ult}$ corresponding to loss of stability of the arch in the NL model,
3. phase III – at force P_{III} level corresponding to reaching by the edge stresses the compressive strength f_c in the EL model.

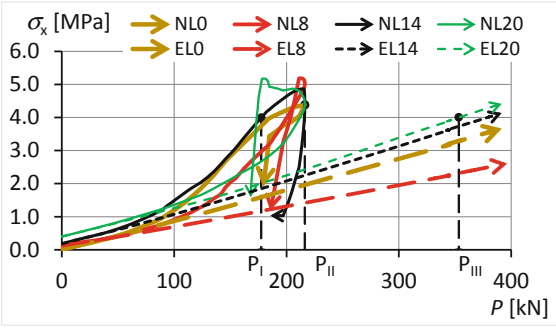

Fig. 3. Relationships between edge stress σ_x in critical sections (nos. 0, 8, 14 & 20) and applied force P for EL and NL models of an arch with: f/L = 1/4 and d = 40 cm

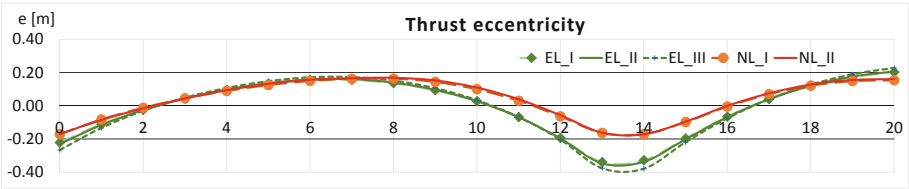

Fig. 4. Distribution of the thrust in phases I-III for EL and NL models of an arch with: *f/L* = 1/4 and *d* = 40 cm

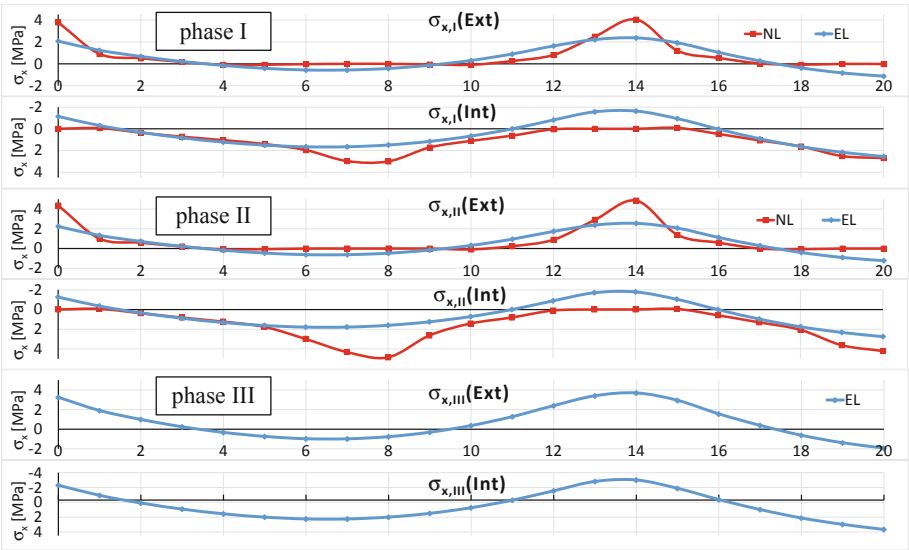

Fig. 5. Distribution of edge stresses in following phases for EL and NL models along extrados (top) and intrados (bottom) of an arch with: *f/L* = 1/4 and *d* = 40 cm

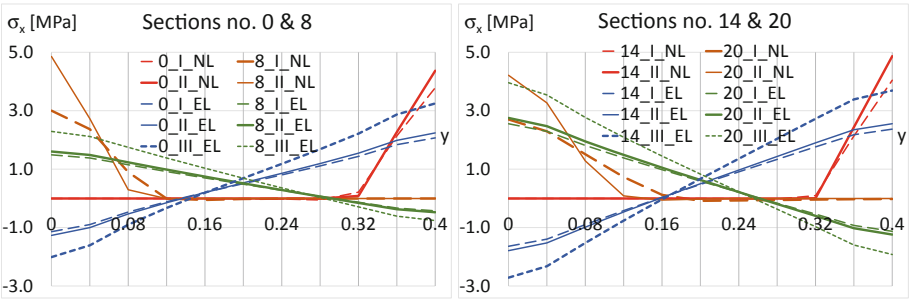

Fig. 6. Distribution of stresses in critical sections in phases I-III for EL and NL models of an arch with: *f/L* = 1/4 and *d* = 40 cm

An effective measure of discrepancy between results obtained by means of the both models may be also expressed on the percentage basis with s parameter comparing edge stresses referred to the material compressive strength according to the formula:

$$s = \frac{\sigma_{EL} - \sigma_{NL}}{f_c}[\%] \tag{1}$$

Results presenting values of s parameter calculated in the phase I for extrados and intrados of all arches considered in the parametric study are given in Fig. 7.

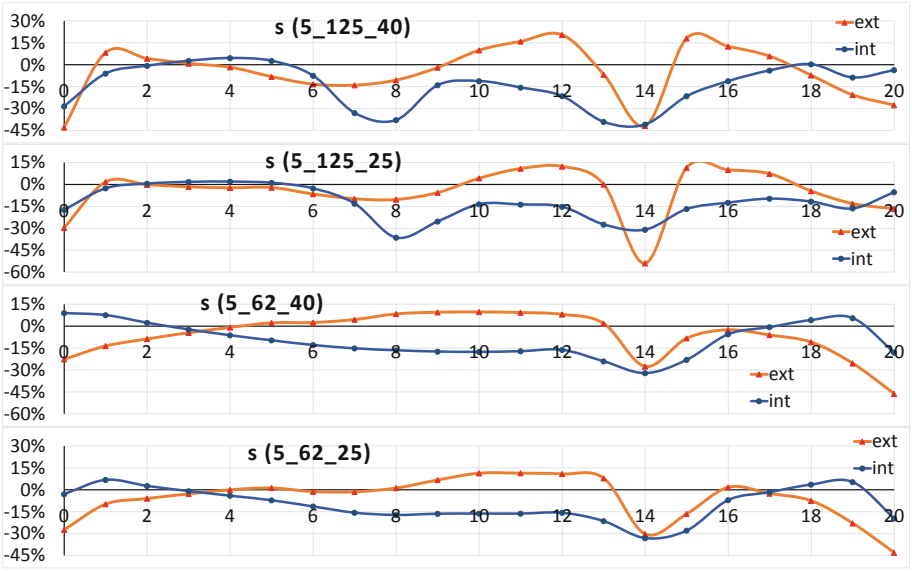

Fig. 7. Relationships between edge stresses in phase I at extrados and intrados for all arch geometries (notation system: *L_r_d*)

4 Analysis of Results

The presented $\sigma(P)$ relationships (Fig. 3) corresponding to both models differ significantly starting from an early phase of live loads. A large difference between values of forces P_{I} and P_{III} corresponding to reaching by the edge stresses the compressive strength f_{c} in the NL and EL models is visible. Moreover, f_{c} is being reached first during the process of loading in different section. For the case presented in Fig. 3 according to NL model the stress equal to f_{c} appear first at section no. 14 while for EL model it takes place in section no. 20. It confirm that the selection of the model not only changes the level of stresses in a given section but also influences redistribution of internal forces within the whole arch.

Analysis of the thrust line location (Fig. 4) exposes the essential meaning of the EL model application which allows a great but unreal eccentricity virtually laying much outside the arch. At the same time in such a model the edge stresses σ_x in critical sections of the arch (see Fig. 5) are much lower than in NL model. However, in some other regions the compressive stresses may be higher for EL than for NL model. Regarding the tensile stresses they are negligibly small in NL model what correctly represents reality while in EL model they become significant reaching 3 MPa in phase III.

Distribution of stresses throughout the whole critical sections (Fig. 6) reveals the huge difference between the models regarding the mechanism of the internal force transmission within the masonry arch. In EL model the bending moment is transferred by partial compression and tension of a section whereas in NL model this response may be generated by eccentrical compression only.

The proposed *s* parameter shows that difference between results generated using EL and NL models gets from −54% up to 20% of the material strength value. In the critical section the difference reaches the most extreme negative values.

Neglecting the material yielding at compression the discrepancy between the both models related to the generated compressive edge stresses is dependent to the size of the thrust eccentricity *e*. If the eccentricity is measured by means of a normalized ratio $k = e/d$, then the discrepancy $f(k)$, defined as a ratio of compressive edge stresses $\sigma_{x,EL}$ determined in EL model to the stresses $\sigma_{x,NL}$ obtained from NL model, may be represented by the diagram given in Fig. 8. As it is shown the function $f(k)$ gets value 1.0 when $k \leq 1/6$, while it drops according to Eq. (1) to zero when $k = 1/2$:

$$f(k) = -9k^2 + 3k + 3/4 \tag{2}$$

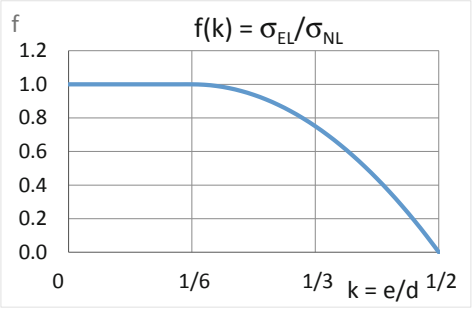

Fig. 8. Ratio of compressive edge stresses σ_x of a section at eccentrical compression determined in EL and NL models as a function of *k* ratio

5 Conclusions

The presented study reveals consequences resulting from selection of a simple linear-elastic model in analysis of masonry arches. It clearly shows that the differences arising from such an approach against the real behaviour of these non-tensile-resistant structures are so large, that the simplification is unacceptable. The agreement between the

EL and NL models covers only the phase of the structure loading until the value of tensile stresses are below the material tensile strength, which however corresponds just to very low level of loads for typical bridges. For most of the structures any exploitation loads related to road or railway traffic lead to exceeding of the tensile strength and consequent discrepancy between the results.

An important finding is that EL models provide lower compressive stresses than NL models do for the given level of a structure load what makes the application of such simplified models in analysis of masonry arch bridges the non-conservative approach which is usually opposite to analysis of other types of structures.

Function $f(k)$ provided in the paper may be a legible measure of the discrepancy between results obtained by means of the both models showing how much the edge stresses calculated by EL model may be lower than those received from NL model.

References

1. UIC Code 778-3R. Recommendations for the assessment of the load carrying capacity of existing masonry and mass-concrete arch bridges (1995)
2. Costa, C., Kamiński, T.: Comparison of various modelling techniques applied in analysis of masonry arch bridges. In: 8th International Conference on Arch Bridges, Wrocław, Poland, 5–7 October 2016, pp. 835–842 (2016)
3. Hojdys, Ł., Kamiński, T., Krajewski, P.: Experimental and numerical simulations of collapse of masonry arches. In: 7th International Conference on Arch Bridges, Trogir-Split, Croatia, pp. 715–722 (2013)
4. Kamiński, T.: Tests to collapse of masonry arch bridges simulated by means of FEM. In: 5th International Conference on Bridge Maintenance. Safety, Management and Life-Cycle Optimization (IABMAS 2010), Philadelphia, USA, pp. 1420–1427. Taylor & Francis Group, London (2010)
5. Kamiński, T., Bień, J.: Condition assessment of masonry bridges in Poland. In: National Conference on Bridge Maintenance and Safety of Bridges (ASCP'2015), 25–26 June 2015, Lisbon, Portugal, pp. 126–135 (2015)
6. Kamiński, T., Machelski, Cz.: Experimental and numerical study on displacements of masonry bridges under live loads. In: 8th International Conference on Arch Bridges, Wrocław, 5–7 October, pp. 1019–1028 (2016)
7. Kamiński, T.: Mesomodelling of masonry arches. In: 6th International Conference AMCM 2008 – Analytical Models and New Concepts in Concrete and Masonry Structures Łódź, Poland, 9–11 June 2008, pp. 359–360 (2008)
8. Kamiński, T., Bień, J.: Application of kinematic method and FEM in analysis of ultimate load bearing capacity of damaged masonry arch bridges. Procedia Eng. **57**, 524–532 (2013)
9. Lee, J.S., Fenves, G.L.: Plastic-damage model for cyclic loading of concrete structures. J. Eng. Mech. **124**(8), 892–900 (1998)
10. Lubliner, J., Oliver, J., Oller, S., Oñate, E.: A plastic-damage model for concrete. Int. J. Solids Struct. **25**(3), 229–326 (1989)
11. Helmerich, R., Niederleithinger, E., Trela, C., Bień, J., Kamiński, T., Bernardini, G.: Multi-tool inspection and numerical analysis of an old masonry arch bridge. Struct. Infrastruct. Eng. **8**(1), 27–39 (2012)